An Optimal Multirate Control Design with Robustness Specification for Sampled-Data HDD Servo Systems

Qi Hao[1], Guoxiao Guo, Ruifeng Chen, Shixin Chen, and Teck-Seng Low

Abstract

One major contributor of the Track Mis-registration (TMR) in an Hard Disk Drive (HDD) servo system is the position error signal (PES) 3σ, or 3 times the standard deviation of the PES. This paper presents an optimal robust multirate control design to minimize $3\sigma_{PES}$ in HDD servo systems with stochastic distribution of plant parameters via genetic algorithm (GA) and random neighborhood search (RNS) considering robust stability restrictions. The expected H_2 norm of the sampled-data system was set as the robust performance index and the H_∞ norm of weighted complementary sensitivity function of the plant input was set as the robust stability index for the multiplicative perturbation. The genetic algorithm with sharing scheme and tabu list which could improve diversity of solutions and global search ability was employed for a coarse optimization of the controller parameters and random neighborhood search did a fine-tuning of the controller. The numerical results show that, the proposed method could improve the robust performance of the sampled-data HDD servo system considerably while keeping the robust stability.

Index Terms— **Multirate, sampled-data system, track mis-registration, genetic algorithm, robust control, HDD servo.**

1 Introduction

One of the prerequisites of moving to higher TPI in HDDs is to improve the servo system performance for lower TMR. A higher track density can only be achieved through a reduction in the total TMR. Usually, TMR is caused by various error sources inside an HDD and could be described as $\pm 3\sigma$ of the offset between the actual head position and track center because of its statistical nature. To cope with the challenge of the actuator pivot nonlinearity, high frequency uncertainty, the effects of various external disturbances and noises, control techniques such as PID, LQG/LTR, H_2/H_∞ and multirate control have been extensively studied and used for HDD servo control ([1], [2], [3], [4]). To increase the closed loop bandwidth while avoiding the amplification of the unwanted noise and disturbances, detailed plant models, including noise, disturbance and uncertain models, have been studied to facilitate the servo controller design.

Like in most control systems, performance and robustness are two vital factors limiting the use of a controller in the commercial mass-produced hard disk drives. Usually, the real time performances require to minimize H_2 norm of some system channels, while robust stability of closed loop system under the action of uncertainty needs keeping bounds on the H_∞ norm of some other channels. Such a multiobjective H_2/H_∞ problem has been proposed and solved by optimization of Youla parameter ([5], [6]) or alternatively through solving Linear Matrix Inequality (LMI) ([7]).

Besides, for the sampled-data HDD servo systems, continuous-time design has the advantage that detailed VCM model, including the flexible modes of the actuator, can be employed. All kinds of continuous-time controller can be designed based on such model for a wide varieties of control objectives. However, unlike most digital control systems where increasing the sampling rate can simply be done by using a faster micro processor, the position information on an embedded HDD is limited. It is because the drive is primary designed for storing user data and not for perfect tracking at all costs. Relatively lower sample rate, therefore, severely limits the direct conversion of controllers designed in continuous time to real drives due to the well known fact that discretization of analog controller is effective only if the sampling rate is high enough.

Digital designs, on the other hand, suffers from the inaccuracy of the plant model, as some of the resonance modes are close to or may fall out of the Nyquist frequency. The digital redesign technique was proposed ([8], [9]) to retain the high bandwidth characteristic of the analog design at a low sample rate. In addition, the direct sampled-data approach has also been proposed to design a digital controller in the continuous-time domain ([10],[11],[12]).

However, as the gain of VCM plant and resonance frequencies in HDD servo systems are quite large and high ($10^7 \mu m/V$ and kHz), from time to time the optimal solution could not be easily obtained through solving a series of Ricatti equations due to the computation instability caused by ill conditions of the problem and the rounding errors. Therefore, in real engineering case, it is appealing and practical to apply some numerical optimization methods to solve the control problem, in which certain control law structure and dynamic order are prescribed and the parameters of control law are optimized considering both robust performance and robust stability of the system ([4], [13], [14], [15], [16], [17]). Among those methods, some random optimization algorithm such as Random Neighborhood Search (RNS), and Genetic Algorithm (GA) are employed for their well known property of robustness to the error of objective function and ability of global search ([1], [15]).

This paper presents a new scheme for synthesizing op-

[1]The authors are with Data Storage Institute, DSI Building, No. 5, Engineering Drive 1, Singapore 117608, Singapore. Phone: (65) 8748500, Fax: (65) 7772053. Email: haoqi, dsiguogx, chenrf, dsicsx, tslow@dsi.nus.edu.sg.

timal sampled-data HDD servo multirate control law using GA and RNS method. A nonlinear cost function was proposed to include expected H_2 norm of system and H_∞ norm of weighted complementary sensitivity function at plant input for optimization. More specifically, the proposed multirate controller was initialized with a structure of multirate LQG controller in series with multirate notch filter and was further re-optimized using a plant possibility model to achieve better performance and robustness as much as possible.

2 Problem Statement

In this section, a sampled-data HDD servo system and a multirate controller structure are presented. The robust performance index and robust stability indexes are defined before identification of a plant with random distribution of parameters as a possibility model.

2.1 Multirate Sampled-Data System Models

The block diagram of multirate stochastic sampled-data HDD servo system is shown in Fig 1. The analog plant augmented with disturbance model is

$$\begin{aligned} \dot{\mathbf{x}}(t) &= \tilde{\mathbf{A}}\mathbf{x}(t) + \tilde{\mathbf{B}}_{w1}w_1(t) + \tilde{\mathbf{B}}_{w2}w_2(t) + \tilde{\mathbf{B}}_u u(t), \\ y(t) &= \mathbf{C}\mathbf{x}(t), \\ y_m(k) &= y(k) + v_d(k). \end{aligned} \quad (1)$$

where $\tilde{*}$ means random variables. $\tilde{\mathbf{A}} \in \mathbf{R}^{n\times n}$, $\tilde{\mathbf{B}}_u$, $\tilde{\mathbf{B}}_{w_1}$, $\tilde{\mathbf{B}}_{w_2}$, $\mathbf{C}^T \in \mathbf{R}^n$ is the general plant model, whose parameters $\theta_p \in \Omega_p$, the space of possible parameter variations. $\mathbf{x}(t) \in \mathbf{R}^n$ is plant and disturbance state. $y(t)$, $y_m(k)$, $u(t) \in \mathbf{R}^1$ are true, measured system output and control. $w_1(t)$, $w_2(t)$, $v_d(k) \in \mathbf{R}^1$ are process and measurement noise respectively, which are modeled as continuous-time unity white noise processes and discrete-time filtered unit white noise process. Usually multirate controllers are adopted to achieve

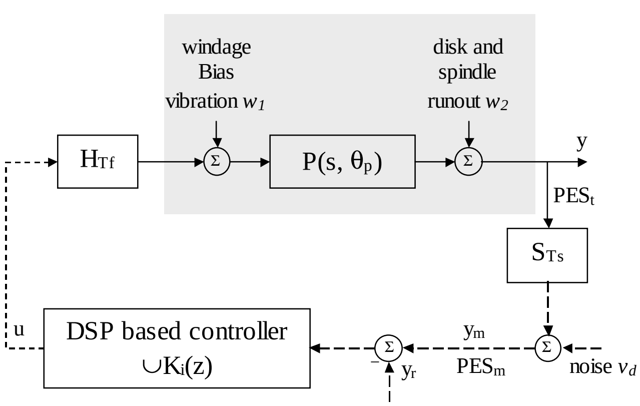

Figure 1: Block diagram of the optimal robust multirate control system.

smoother control behavior and less sensitivity to disturbance/noise. In this paper, a multirate LQG controller plus a multirate notch filter is used, in which r sets of state feedback gains and estimation gains $\bigcup_{i=1}^{r}(\mathbf{K}_i, \mathbf{L}_i)$ are adjustable parameters, with control update period $T_f = T_s/r$. Such a periodically time-varying SISO controller could be equivalent to a lifted time-invariant SIMO one with update period T_s as

$$\begin{aligned} \hat{\mathbf{x}}(k+1) &= \mathbf{\Phi}_c\hat{\mathbf{x}}(k) + \mathbf{\Gamma}_c(y_m(k) - y_r), \\ \mathbf{u}(k) &= \mathbf{H}_c\hat{\mathbf{x}}(k), \end{aligned} \quad (2)$$

where

$$\mathbf{\Phi}_c = \begin{bmatrix} \mathbf{\Phi}_g & \mathbf{0} & \mathbf{0} & \dots & \mathbf{0} \\ \mathbf{\Gamma}_{h1}\mathbf{K}_1 & \mathbf{\Phi}_{h1} & \mathbf{0} & \dots & \mathbf{0} \\ \vdots & & \dots & & \\ \mathbf{\Gamma}_{hr}\mathbf{K}_r & \mathbf{0} & \dots & \mathbf{0} & \mathbf{\Phi}_{hr} \end{bmatrix} \in \mathbf{R}^{m\times m}$$

$$\mathbf{\Gamma}_c^T = [\mathbf{\Gamma}_g^T \;\; \mathbf{0} \;\; \dots \;\; \mathbf{0}] \in \mathbf{R}^{1\times m}$$

$$\mathbf{H}_c = \begin{bmatrix} \mathbf{J}_{h1}\mathbf{K}_1 & \mathbf{H}_{h1} & \mathbf{0} & \dots & \mathbf{0} \\ \vdots & & \dots & & \\ \mathbf{J}_{hr}\mathbf{K}_r & \mathbf{0} & \dots & \mathbf{0} & \mathbf{H}_{hr} \end{bmatrix} \in \mathbf{R}^{r\times m}$$

$$\mathbf{\Phi}_g = \bar{\mathbf{\Phi}}_s - \sum_{i=1}^{r} \bar{\mathbf{\Phi}}_f^{r-i}(\bar{\mathbf{\Gamma}}_{uf}\mathbf{K}_i + \mathbf{L}_i\bar{\mathbf{C}}) \in \mathbf{R}^{n\times n}$$

$$\mathbf{\Gamma}_g = \sum_{i=1}^{r} \bar{\mathbf{\Phi}}_f^{r-i}\mathbf{L}_i\bar{\mathbf{C}} \in \mathbf{R}^n$$

$\bar{\mathbf{\Phi}}_s = e^{\bar{\mathbf{A}}T_s} \in \mathbf{R}^{n\times n}$, $\bar{\mathbf{\Phi}}_f = e^{\bar{\mathbf{A}}T_f} \in \mathbf{R}^{n\times n}$, $\bar{\mathbf{\Gamma}}_{uf} = \int_0^{T_f} e^{\bar{\mathbf{A}}\tau}\mathbf{B}_u d\tau \in \mathbf{R}^n$. $(\bar{\mathbf{A}}, \bar{\mathbf{B}}, \bar{\mathbf{C}})$ is the continuous-time nominal plant model compensated by a notch filter. $(\mathbf{\Phi}_{hi}, \mathbf{\Gamma}_{hi}, \mathbf{H}_{hi}, \mathbf{J}_{hi})$ is the *ith* notch filter for the *ith* multirate control. $\hat{\mathbf{x}}(k) \in \mathbf{R}^m$ is controller state and $y_r \in \mathbf{R}^1$ is the reference ([4], [19]).

2.2 Robust Performance

The objective of the track following servo control is to maintain a minimum tracking error. This problem normally is solved by using standard methods such as pole placement, LQG/LTR, H_2/H_∞ ([2], [3], [4]), etc, based on a nominal plant model. Such controllers, when combined with proper seeking controllers and mode switching mechanism ([18]), can make sure that the disk drive read/write head reach a desired track quickly and remain on the track accurate enough for reliable read and write.

However, since the actuator parameter and disturbance model variations are very common under different operation conditions for the disk drives, the control design based on nominal plant models may not be suitable to achieve the best robust performance. In our study, the stochastic plant was identified as several linear models, each of which was given a discrete possibility. The true TMR, defined statistically as the $\pm 3\sigma$ of true position error signal (PES) $\mathbf{e}$, was chosen as the robust performance index for a direct optimization of the HDD servo controller.

If the models of disturbances and noise are pre-known, then to a plant with known parameter distribution the deviation of true PES could be obtained as the expected H_2 norm of the transfer function from unit white noise processes, sources of disturbances and measurement noises, to plant output $\tilde{\mathbf{T}}_{yw}$ and $\tilde{\mathbf{T}}_{yv_d}$, that is

$$\sigma_{ee} = [\frac{1}{T_s}E\{\|\tilde{\mathbf{T}}_{yw}\|_2^2 + \|\tilde{\mathbf{T}}_{yv_d}\|_2^2\}]^{\frac{1}{2}} \quad (3)$$

The coefficient $\sqrt{\frac{1}{T_s}}$ before H_2 norm of sampled-data system is due to the definition of H_2 norm of sampled-data system and will be explained further in Appendix.

2.3 Robust Stability

Beside the requirement on dynamic performance, the robust stability is usually required for control design. A realistic way to express plant uncertainty is to describe the plant transfer function as having a multiplicative uncertainty as

$$\tilde{\mathbf{P}} = \{\mathbf{P}(1+\mathbf{\Delta W}_\delta) : \|\mathbf{\Delta}\|_\infty < 1\} \quad (4)$$

where the causal, stable and fixed weighting system $\mathbf{W}_\delta$ models uncertainty envelope in the magnitude of the plant, and $\mathbf{\Delta}$ models uncertainty in the phase.

As it follows, an upper bound on the stability margin is

$$\gamma_{rs} = 1/\|\mathbf{W}_\delta \mathbf{S}_i\|_\infty \quad (5)$$

where $\mathbf{S}_i$ is the complementary sensitivity function of plant input ([10], [20]).

2.4 Stochastic Plant Identification

To a plant set with randomly distributed parameters $\mathbf{P}(\theta_p)$, where all the parameters are independent random variables, one way to achieve the robust performance of system is to evaluate the performance of several sampled plants from the plant set, each of which is given a reasonable possibility. The possibilities for N sampled plants could be written as

$$\begin{aligned} \rho_1 &= sin^2\eta_1, \\ \rho_2 &= cos^2\eta_1 sin^2\eta_2, \\ &\dots \\ \rho_{N-1} &= cos^2\eta_1 cos^2\eta_2 \dots cos^2\eta_{N-2} sin^2\eta_{N-1}, \\ \rho_N &= cos^2\eta_1 cos^2\eta_2 \dots cos^2\eta_{N-2} cos^2\eta_{N-1}, \end{aligned} \quad (6)$$

where $\eta_1, \dots, \eta_{N-1} \in [0, \pi/2]$. Thus the identification problem becomes a nonlinear optimization problem:

$$(\eta_1, \dots, \eta_{N-1}, \theta_{p1}, \dots, \theta_{pN}) = arg \min_{\eta, \theta_p} J(\mathbf{R}_{uu}(z), \mathbf{R}_{yy}(z)) \quad (7)$$

where $\mathbf{R}_{uu}(z)$ and $\mathbf{R}_{yy}(z)$ are the power spectrum of system input and output.

3 Equivalence of the Multirate Sampled-data System

For the HDD servo system, the performance index, true TMR, is the root-mean-square (RMS) of the continuous-time plant output other than that of the sampled plant output. Using the continuous lift technique, which can reduce the hybrid continuous/discrete-time problem to a norm-equivalent discrete-time problem, both the intersample behavior of the system and the effect of the sampling frequency on the performance could be taken into estimation ([10],[11]). An equivalent time-invariant discrete plant can be obtained as

$$\begin{aligned} \bar{\mathbf{x}}(k+1) &= \tilde{\mathbf{\Phi}}_s \bar{\mathbf{x}}(k) + \tilde{\mathbf{\Gamma}}^*_{w_1 s} w_1(k) + \tilde{\mathbf{\Gamma}}^*_{w_2 s} w_2(k) + \tilde{\mathbf{\Gamma}}^*_{us} \bar{\mathbf{u}}(k), \\ \bar{\mathbf{y}}(k) &= \mathbf{H}_s \bar{\mathbf{x}}(t) + \tilde{\mathbf{J}}_{us} \bar{\mathbf{u}}(k), \\ \bar{y}_m(k) &= [1\ 0\ \dots\ 0]\bar{\mathbf{y}}(k) + v_d(k). \end{aligned} \quad (8)$$

where

$$\tilde{\mathbf{\Phi}}_s = e^{\tilde{\mathbf{A}} T_s} \in \mathbf{R}^{n\times n}$$

$$\tilde{\mathbf{\Gamma}}^*_{ws} \tilde{\mathbf{\Gamma}}^{*T}_{ws} = \int_0^{T_s} e^{\tilde{\mathbf{A}}\tau} \tilde{\mathbf{B}}_w \tilde{\mathbf{B}}_w^T e^{\tau \tilde{\mathbf{A}}^T} d\tau \in \mathbf{R}^{n\times n}$$

$$\tilde{\mathbf{\Gamma}}^*_{us} = [\tilde{\mathbf{\Phi}}_f^{r-1} \tilde{\mathbf{\Gamma}}_{uf}\ \dots\ \tilde{\mathbf{\Phi}}_f \tilde{\mathbf{\Gamma}}_{uf}\ \tilde{\mathbf{\Gamma}}_{uf}] \in \mathbf{R}^{n\times r}$$

$$\tilde{\mathbf{\Gamma}}_{uf} = \int_0^{T_f} e^{\tilde{\mathbf{A}}\tau} \tilde{\mathbf{B}}_u d\tau \in \mathbf{R}^n$$

$$\tilde{\mathbf{\Phi}}_f = e^{\tilde{\mathbf{A}} T_f} \in \mathbf{R}^{n\times n}$$

$$\mathbf{H}_s^T = [\mathbf{H}_f^{*T}\ \tilde{\mathbf{\Phi}}_f^T \mathbf{H}_f^{*T}\ \dots\ \tilde{\mathbf{\Phi}}_f^{T(r-1)} \mathbf{H}_f^{*T}] \in \mathbf{R}^{n\times r(n+1)}$$

$$\tilde{\mathbf{J}}_{us} = \begin{bmatrix} \tilde{\mathbf{J}}^*_{uf} & \mathbf{0} & \dots & \mathbf{0} \\ \mathbf{H}^*_f \mathbf{\Gamma}_{uf} & \tilde{\mathbf{J}}^*_{uf} & \dots & \mathbf{0} \\ \vdots & & \ddots & \\ \mathbf{H}^*_f \mathbf{\Phi}_f^{r-2} \mathbf{\Gamma}_{uf} & \dots & \mathbf{H}^*_f \mathbf{\Gamma}_{uf} & \tilde{\mathbf{J}}^*_{uf} \end{bmatrix} \in \mathbf{R}^{r(n+1)\times r}$$

$$[\mathbf{H}^*_f\ \tilde{\mathbf{J}}^*_{uf}]^T [\mathbf{H}^*_f\ \tilde{\mathbf{J}}^*_{uf}] = \int_0^{T_f} e^{\tilde{\underline{\mathbf{A}}}\tau} [\mathbf{C}\ \ 0]^T [\mathbf{C}\ \ 0] e^{\tau \tilde{\underline{\mathbf{A}}}^T} d\tau \in \mathbf{R}^{(n+1)\times(n+1)}$$

$$\tilde{\underline{\mathbf{A}}} = \begin{bmatrix} \tilde{\mathbf{A}} & \tilde{\mathbf{B}}_u \\ \mathbf{0} & \mathbf{0} \end{bmatrix} \in \mathbf{R}^{(n+1)\times(n+1)}$$

$$\mathbf{H}^*_f \in \mathbf{R}^{(n+1)\times n},\ \tilde{\mathbf{J}}^*_{uf} \in \mathbf{R}^{(n+1)}$$

The H_2 norms of the two system in (1) and (8) satisfy

$$\|\tilde{\mathbf{T}}_{ywv}\|_2^2 = \|\tilde{\mathbf{D}}\|_{HS}^2 + \|\tilde{\mathbf{T}}_{\bar{y}wv}\|_2^2 \quad (9)$$

where

$$\|\tilde{\mathbf{D}}\|_{HS}^2 = trace\{\tilde{\mathbf{B}}_w^T \int_0^{T_s} \int_0^t e^{\tau \tilde{\mathbf{A}}^T} \mathbf{C}^T \mathbf{C} e^{\tilde{\mathbf{A}}\tau} d\tau dt \tilde{\mathbf{B}}_w\}$$

is the $Hilbert-Schmidt$ norm and is irrelevant with controller. Therefor the H_2 optimal controller for system in (8) is the same for the original system in (1).

4 Optimization Algorithm

In this section, GA with sharing scheme/tabu list and RNS method are briefly introduced. A nonlinear cost function for optimization is defined before the whole design procedure is summarized.

4.1 Genetic Algorithm and RNS

Genetic algorithm (GA) is a kind of discrete-time Markoff chain converging to the minima of performance surface ([21]). GAs work by employing populations of structures (called chromosomes) that encode candidate solution for a problem into binary strings. These structures are allowed to undergo changes by means of so-called genetic operators, chiefly *crossover*, *mutation* and *selection*, which encourages reproduction of some characteristics from those individuals with better performance.

One of the most pervasive problems existed in GA is that of premature convergence of the process, almost invariably associated with a loss of diversity. This problem is especially critical to multimode (multi-minimum) function optimization. Some methods, inspired by a natural notion of niche and species, have been proposed to alleviate the problem, such as *preselection*, *crowding scheme*, *sharing scheme* and *tabu list* ([21], [22]). The central idea of sharing scheme is to enforce the individuals of the population to share available resources by dividing the population into different subpopulation on the basis of similarity of chromosomes.

To implement the sharing scheme, a simple linear function called sharing function $Sh(d^{ij})$ is adopted as a function of the distance between two chromosomes d^{ij}. The sharing function is evaluated for each pair of chromosomes in the population, and then the sum $Sh^j = \sum_i Sh(d^{ij})$ is computed for the jth chromosome. Finally, the fitness of this chromosome is adjusted by dividing by Sh^j. Using a tabu list, which keeps tracks of recent solutions, could incorporate a short-term memory into a GA and thus keep a search from being trapped in a local minimum. More details could be found in [22].

However, due to the limitation of computation time and the huge search space of our problem that for a 4^{th}-order plant with double rate control at least 16 controller parameters need to be optimized, we use another random optimization method random neighborhood search (RNS) to fine tune the solution obtained from above GA.

RNS is a type of Monte Carlo procedure with an improved technique for choosing parameters. Although its implementation only need a few line codes, it can effectively search a region in parameter space centered on a point which has the lowest known cost ([1]). With the combination of GA and RNS, we could both search a large parameter space for a global optimal solution and obtain a fine tuned resultant controller.

4.2 Cost Function

A nonlinear robustness cost function was set as:

$$J = \begin{cases} \sigma_{ee} + 1/\gamma_{rs}, & if \;\; \gamma_{rs} < 1 \\ \sigma_{ee}, & if \;\; \gamma_{rs} \geq 1 \end{cases} \tag{10}$$

For GA, such a cost function had to be transformed and rescaled to get the fitness function.

4.3 Summary

As a summary, the following steps were adopted to find an optimal controller.

Step1 : Collect the experimental data on a large quantity basis to find the bounds of plant model uncertainty and parameter distribution, as well as disturbance/noise model.
Step2 : Identify the stochastic plant model as several continuous-time models each with discrete possibility using (7).
Step3 : Obtain an initial controller with enough stability margin using ordinary multirate LQG design techniques and define a large controller parameter space on the basis of the initial controller parameter values.
Step4 : Run the GA optimization routine to minimize the cost function (10), searching for the location of global optimal parameters of controller with structure of (2).
Step5 : Tune the controller parameters with RNS method for a local search.
Step6 : Repeat step 4, 5 until there is no significant improvement in the cost function.

It could be noted that the GA does not guarantee the solution it obtains within limited computation time is global optimal, thus several repetitions of whole optimization process would bring us more chance to get a better solution.

5 An Application Example

In this section, the design method given in the previous sections will be applied to a disk drive servomechanism.

5.1 Plant, Uncertainty and Noise Models

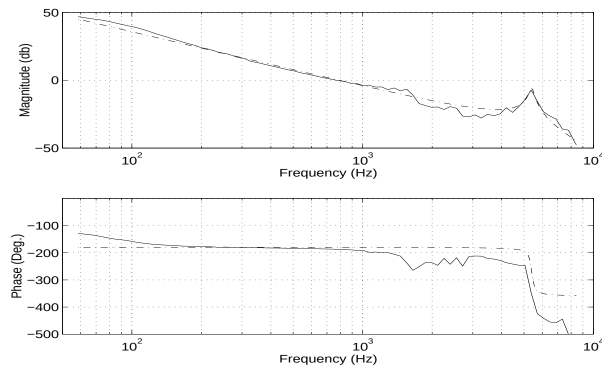

Figure 2: Bode plot of an HDD actuator.

In an HDD servo control system, the plant model is usually considered as a double integrator together with resonance modes. A measured Bode diagram of the real HDD (actuator plus power amplifier) is shown as the solid line in Fig. 2. The dash-dot line was the identified plant model with a transfer function form of

$$\frac{Y(s)}{U(s)} = \frac{\omega_n^2}{s^2 + 2\zeta_n \omega_n s + \omega_n^2} \frac{k}{s^2}, \tag{11}$$

where $k = 2.41 \times 10^7 \mu$m/V$\pm35\%$ was the plant gain, $\omega_n = 5400$ Hz$\pm10\%$, $\zeta_n = 0.04\pm40\%$. The sampling frequency was 14 kHz.

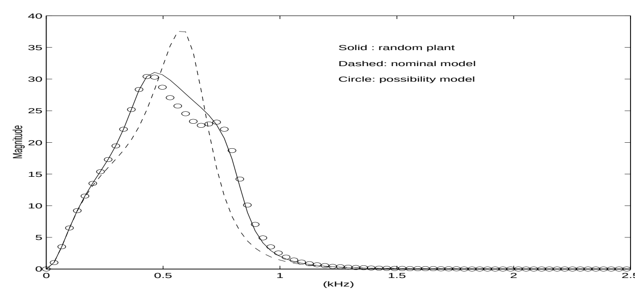

Figure 3: Power spectrum of PES caused by a unit white noise before plant.

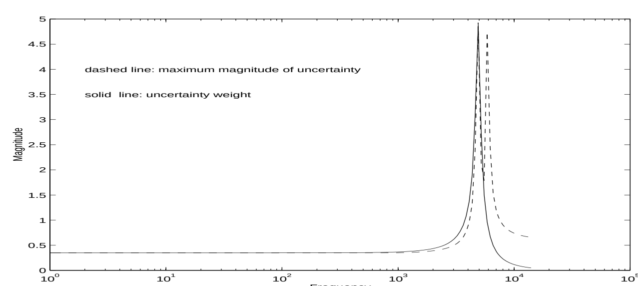

Figure 4: Uncertainty of the plant and uncertainty weight.

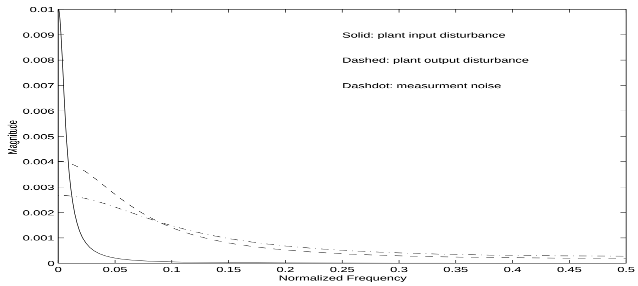

Figure 5: Disturbance and noise model.

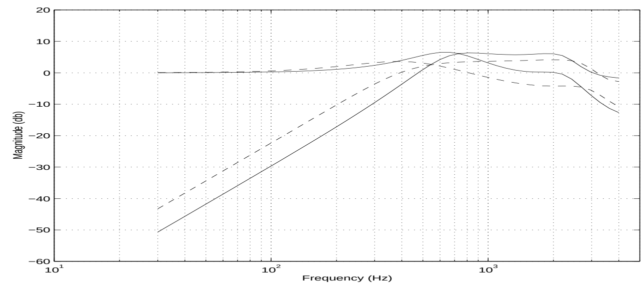

Figure 6: Bode plots of the control system.

For a plant with randomly distributed parameters, it could be identified as several continuous-time models each with a discrete possibility to achieve a satisfying model errors. Fig. 3 shows using 5 plant models could get a good model errors for PID control system.

From Fig. 4 we can find that the maximum magnitude of multiplicative uncertainty obtained by (4) has two peaks, one at 4.9 kHz and another at 5.9 kHz. Since the resonance frequency was 5.4 kHz, only the first peak might destroy the system stability and such that uncertainty weighting model just describing the first peak was selected to reduce the computation. Fig. 5 illustrates the disturbance before and after plant and measurement noise models. All of them were simplified as 1^{st}-order low-pass systems.

5.2 Optimization Settings

The controller parameter space was defined on the basis of multirate LQG controller parameter values. The initial multirate state feedback gains could be obtained through MATLAB function $\mathbf{K}_0 = dlqry(\bar{\mathbf{\Phi}}_s, \bar{\mathbf{\Gamma}}^*_{us}, \bar{\mathbf{C}}, \mathbf{0}, \mathbf{Q}, \mathbf{R})$. $\mathbf{Q}$ and $\mathbf{R}$ were weighting factor/matrix. The initial multirate estimator gains could be obtained ([19]) by

$$\mathbf{L}_i = \Big(\sum_{i=1}^{r} \bar{\mathbf{\Phi}}^i_f\Big)^{-1} \bar{\mathbf{\Phi}}_s \mathbf{L}_0$$

where $\bar{*}$ meant plant model after notch filter compensation. $\mathbf{L}_0 = dlqe(\bar{\mathbf{\Phi}}_s, \bar{\mathbf{\Gamma}}_{us}, \bar{\mathbf{C}}, \mathbf{W}, \mathbf{V})$. $\mathbf{W}$ and $\mathbf{V}$ were the power of disturbance and noise.

Using double-rate LQG structure, 16 controller parameters were encoded as a 192-bit string. The population size $N = 200$, number of generation $gen = 100$, crossover possibility $P_c = 0.95$, and mutation possibility $P_m = 0.1$. The sharing parameter phenotypic $\sigma_{sh} = 0.05 \times [\mathbf{K}_{i0}\mathbf{L}_{i0}]$, and the length of tabu list was N.

5.3 Optimization Results

The sensitivity and complimentary sensitivity Bode plots of double-rate LQG control system and optimized control system are shown as dashed and solid lines in Fig. 6. And the weighted complimentary sensitivity function of optimized control system is shown in Fig. 7 to illustrate the robust stability margin. It could be noted that these Bode plots only proximately reflected the characteristics of real sampled-data system, since all of them were based on a pure discrete-time system after step-invariant transform.

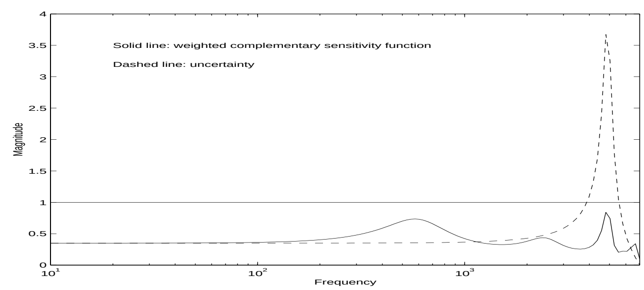

Figure 7: Robust stability margin.

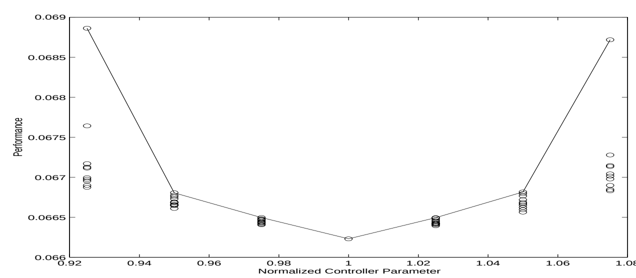

Figure 8: Performance surface near the optimal solution.

Fig. 8 shows the performance surface within the neighborhood of optimal controller. Tab. 1 shows a comparison of robust performances and robust stability upper bound of two control system. The robust performance, PES deviation or expected H_2 norm of system, of the LQG controller and the optimized controller were 0.0821 and 0.0662. The tracking precision was improved by 19.37% while keeping the robust stability.

	LQG control	Optimized control
σ_{ee}	0.0821	0.0662
γ_{rs}	1.0168	1.0444
HS norm	0.0236	0.0236

Tab. 1 Comparison of LQG control and optimized control.

6 Conclusion

In this paper, an optimal robust multirate control design for sampled-data HDD servo systems is presented subject to random fluctuations of plant parameters. A perturbation of LQG problem controller is modified using a genetic algorithm in conjuction with a random neighborhood search to fine tune the controller in a cost of expected H_2 norms and H_∞ norm of system. For a specific HDD servo system, after the optimization, the performance was improved by 19.37% while the required robust stability was kept compared with ordinary multirate LQG control. From the numerical results, we may conclude that the proposed method is practical and effective for the control design of the small inertia plants like VCM.

7 APPENDIX

H_2 norm of hybrid system

Usually, the H_2 norm of a LTI system could be obtained from the 2-norm of the impulse response signal. It also equals the expected RMS of the system output, when system input is a unit variance white noise process [20]. For the periodically time-varying sampled-data system, shown in Fig. 9, the *generalized* H_2 *measure* is defined by $Hilbert-Schmidt$ norm ([10]) as

$$J = \Big(\int_0^{T_S} \sum_i \|\mathbf{T}_{zw}\delta_\tau \mathbf{e}_i\|_2^2 d\tau\Big)^{\frac{1}{2}} \tag{12}$$

where $\delta_\tau(t) = \delta(t-\tau)$, $\mathbf{e}_i$ is the ith standard basis vector. Thus, the expected RMS of the system output corresponding to the unit white noise process input should be $J/\sqrt{T_s}$. In addition, the power spectrum of the signal applied to the analog plant caused by a continuous-time unit white noise process $w(t)$ is $\mathbf{1}(\omega)$ and that caused by a discrete-time white noise $w_d(t)$ is $T_f sinc^2(\frac{\omega T_f}{2})$. Therefore the RMS of sampled system output $y_m(t)$ corresponding to the latter will approximately be $\sqrt{T_f}$ times of that to the former, when the sampling frequency is much larger than the system bandwidth. From above analysis, the H_2 norms of hybrid

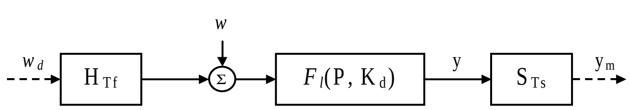

Figure 9: Hybrid System.

system in Fig. 9 satisfy the following relationship,

$$\lim_{T_s\to 0}\|\mathbf{T}_{y_m w_d}\|_2 = 1/\sqrt{T_s}\lim_{T_s\to 0}\|\mathbf{T}_{y w_d}\|_2$$
$$= \sqrt{T_f}\lim_{T_s\to 0}\|\mathbf{T}_{y_m w}\|_2 = \sqrt{T_f}/\sqrt{T_s}\|\mathbf{T}_{yw}\|_2. \tag{13}$$

References

[1] G. F. Franklin, J. D. Powell, and M. L. Workman, *Digital control of dynamic systems*, Addison-Wesley Publishing Company, Reading, MA, 1990.

[2] C. Lin, G. Guo, B. M. Chen, and C. C. Ko, "Optimal track following control for hard disk drives," *Proc. 6th Inter. Workshop on Advanced Motion Control*, p. 502-506, March, 2000.

[3] B. M. Chen, T. H. Lee, C. C. Hang, Y. Guo, and S. Weerasooriya, "An H_∞ almost disturbance decoupling robust controller design for a piezoelectric bimorph actuator with hysteresis," *IEEE Trans. on Control Systems Technology*, vol. 7, no.2, p. 160-174, 1999.

[4] R. Chen, G. Guo, T. Huang, and T.-S. Low, "Optimal multirate control design for hard disk servo system," *IEEE Trans. on Magnetics*, vol. 34, no. 4, p. 1898-1990, July, 1998.

[5] M. Sznair, "An exact solution to general SISO mixed H_2/H_∞ via convex optimization," *IEEE Trans. on Automat. Contr.*, vol. 39, no. 12, p. 2511-2517, Dec., 1994.

[6] C. W. Scherer, "Mulitiobjective H_2/H_∞ Control," *IEEE Trans. on Automat. Contr.*, vol. 40, no. 6, p. 1054-1062, April, 1995.

[7] E. Rijanto, "Quasi mixed H_2/H_∞ controller for a high precision positioning Device," *Proc. 6th Inter. Workshop on Advanced Motion Control*, p. 335-338, March, 2000.

[8] N. Rafee, T. Chen, and O. P. Malik, "A technique for optimal digital redesign of analog controllers," *IEEE Trans. on Control Systems Technology*, vol. 5, No. 1, p. 89-99, 1997.

[9] Y. N. Rosenvasser, K. Yu. Polyakov, and B. P. Lampe, "Application of Laplace transformation for digital redesign of continuous control systems," *IEEE Trans. on Automat. Contr.*, vol. 44, no. 4, p. 883-886, April, 1999.

[10] T. Chen and B. Francis, *Optimal sampled-data control Systems*, Springer-Verlag, Reading, 1996.

[11] L. Qiu and K. Tan, "Direct state space solution of multirate sampled-data H_2 optimal control," Automatica, vol. 34, No. 11, p. 1431-1437, 1998

[12] M.F. Sagfors, H. T. Toivonen and B. Lennartson, "H_∞ control of multirate sampled-data systems: a state-space approach," Automatica, vol. 34, No. 4, p. 415-428, 1998

[13] G. Guo, R. Chen, T.-S. Low, and Y. Wang, "An optimal robust control design for HDD servo systems," *Technical Report*, Data Storage Institute, 1999.

[14] Q. Hao, G. Guo, R. Chen, S. Chen, and T. Low "TMR online optimization using quasi-newton method for HDD servo systems," *Proc. American Control Conference*, P. 3412-3416, June, 2000.

[15] C. I. Marrison and R. F. Stengel, "Robust control system design using random search and genetic algorithm," *IEEE Trans. on Automat. Contr.*, vol. 42, no. 6, p. 835-839, June, 1997.

[16] M. Paskota, V. Sreeram, K. L. Hon, and A. I. Mees, "Optimal simultaneous stabilization of linear single-input systems via linear state feedback control," *International Journal of Control*, vol. 60, no.4, p. 483-498, 1994.

[17] P. A. Weaver and R. M. Ehrlich, "The use of multirate notch filters in embedded-servo disk drives," *Proc. American Control Conference*, p. 4156-4160, June, 1993.

[18] T. Yamaguchi, H. Numasato, and H. Hirai, "A mode-switching control for motion control and its application to disk drives: design of optimal mode-switching conditions," *IEEE/ASME Trans. on Mechatronics*, vol. 3, No. 3, pp. 202-209, Sept. 1998.

[19] T. Hara and M. Tomizuka, "Performance enhancement of multi-rate controller for hard disk drives," *IEEE Trans. on Magnetics*, vol. 35, no. 2, p. 898-903, March, 1999.

[20] K. Zhou and J. C. Doyle, *Essentials of robust control*, Prentice Hall, Reading, NJ, 1998.

[21] G. Chen, *Genetic algorithm and their applications*, People Post, Reading, Beijing, 1996.

[22] Q. Hao, "A genetic algorithm with tabu list and sharing scheme for optimal design of electrical machines," *Elect. Machines and Power Sys.*, vol. 27, no. 5, May, 1999.